

INFORMATION TO USERS

This manuscript has been reproduced from the microfilm master. UMI films the text directly from the original or copy submitted. Thus, some thesis and dissertation copies are in typewriter face, while others may be from any type of computer printer.

The quality of this reproduction is dependent upon the quality of the copy submitted. Broken or indistinct print, colored or poor quality illustrations and photographs, print bleedthrough, substandard margins, and improper alignment can adversely affect reproduction.

In the unlikely event that the author did not send UMI a complete manuscript and there are missing pages, these will be noted. Also, if unauthorized copyright material had to be removed, a note will indicate the deletion.

Oversize materials (e.g., maps, drawings, charts) are reproduced by sectioning the original, beginning at the upper left-hand corner and continuing from left to right in equal sections with small overlaps. Each original is also photographed in one exposure and is included in reduced form at the back of the book.

Photographs included in the original manuscript have been reproduced xerographically in this copy. Higher quality 6" x 9" black and white photographic prints are available for any photographs or illustrations appearing in this copy for an additional charge. Contact UMI directly to order.

UMI

A Bell & Howell Information Company
300 North Zeeb Road, Ann Arbor MI 48106-1346 USA
313/761-4700 800/521-0600



National Library
of Canada

Acquisitions and
Bibliographic Services

395 Wellington Street
Ottawa ON K1A 0N4
Canada

Bibliothèque nationale
du Canada

Acquisitions et
services bibliographiques

395, rue Wellington
Ottawa ON K1A 0N4
Canada

Your file Votre référence

Our file Notre référence

The author has granted a non-exclusive licence allowing the National Library of Canada to reproduce, loan, distribute or sell copies of this thesis in microform, paper or electronic formats.

The author retains ownership of the copyright in this thesis. Neither the thesis nor substantial extracts from it may be printed or otherwise reproduced without the author's permission.

L'auteur a accordé une licence non exclusive permettant à la Bibliothèque nationale du Canada de reproduire, prêter, distribuer ou vendre des copies de cette thèse sous la forme de microfiche/film, de reproduction sur papier ou sur format électronique.

L'auteur conserve la propriété du droit d'auteur qui protège cette thèse. Ni la thèse ni des extraits substantiels de celle-ci ne doivent être imprimés ou autrement reproduits sans son autorisation.

0-612-33415-5

Canada

“ ENERGY STATES OF A HYDROGEN ATOM PLACED BETWEEN TWO METAL SLABS .” a dissertation prepared by Gary McNeill in partial fulfillment of the requirements for the degree, Master of Science , has been approved and accepted by the following:

Dr. V. V. Paranjape

Thesis Advisor

ACKNOWLEDGMENTS

This thesis is dedicated to my mother, Marie, who has taught me the qualities of hard work and perseverance.

I would like to thank the faculty of the Physics Dept., especially Dr. V.V. Paranjape, whose guidance and patience has made this thesis possible.

ABSTRACT

ENERGY STATES OF A HYDROGEN ATOM PLACED BETWEEN TWO METAL SLABS

BY

GARY MCNEILL ©

Master of Science

Lakehead University

Thunder Bay, Ontario

Canada, 1997

In this thesis, we utilize the hydrodynamical model to evaluate the potential energy and self-energy for an electron and a hydrogen atom placed between two semi-infinite metal slabs. The potentials and self-energies are obtained by taking into account the dispersion of the surface plasmons and the effect of confinement by the metal slabs.

Contents

1 INTRODUCTION	1
2 HAMILTONIAN	7
3 POTENTIAL ENERGIES	15
3.1 Results	19
4 ENERGY STATES OF A HYDROGEN ATOM	25
4.1 Ground State	25
4.2 The 3S, 10S and 14S Excited States	29
4.3 Results	30
5 CONCLUDING REMARKS	37
A Hydrodynamical Model	38
B Interaction Energy Integrals	45

1 INTRODUCTION

The interaction energy of an atom with a solid surface, as a function of its position, is of crucial importance in the analysis of various processes which occur at or near a solid-vacuum interface. Some of these processes, among many, include the atomic adsorption (which is of interest to this thesis), surface induced chemical reactions and the scattering of an atom by a surface. The interaction energy, which arises partly as a result of self-induced polarizations of the atom and the surface, is often referred to as the self-energy of the atom. Although studied over a century, a reasonably accurate evaluation of the self-energy came about thirty years ago with the development of what is now known as the density functional theory [1]. The theory, although highly successful, is based heavily on numerical computations in which the physical picture is often blurred. Various approximate approaches [2, 3] in the investigation of surface properties are proposed and discussed regularly in the physics literature. These approaches are not only easy to follow because of their relative simplicity, they are known to offer a credible guidance in the interpretation of experimental results and provide a reasonably good approximation to the results obtained using a more exact theory. These approximate methods have indeed generated a strong following because of the useful role they have played in the development of the subject. One such approach, which we present and utilize in this thesis, is known as the hydrodynamical model. It was initiated a long time

ago by Bloch [4] and is thoroughly discussed in a classic paper by Barton [5]. In this model, the many body properties of the metal electrons are interpreted in terms of longitudinal plasmon modes which are known to exist on the surface and in the bulk of the metal. The dominant interaction between the atom and the surface is assumed to occur as a result of the excitation of the real or virtual surface plasmons by the atom.

In the hydrodynamical theory, (the sketch of which is given in Appendix A), the nuclear charge of the metal is assumed to be static and uniformly smeared over the entire crystal. The electronic charge on the other hand, is represented by a mobile fluid spread over the positively charged background. The fluid motion, governed by the equation of motion and by the requirement of the fluid continuity, can be expressed in terms of collective normal modes described as the bulk and surface plasmons. The bulk modes extend throughout the crystal and possess a uniform amplitude. The surface modes as the name implies, occur on the surface and their amplitude falls exponentially away from the surface. In the use of the plasmon model it is common practice to neglect the dispersion of both surface and bulk plasmon modes and to assume the plasmon frequencies to be independent of the wave vectors. However, these frequencies are known to become dependent on the wave vectors if we include in the equation of motion, (of the electronic fluid), the effect of the pressure exerted by the electron gas. The effect of the pressure on the plasmon frequency as shown in Appendix A is significant only for large values of the wave vectors. At sufficiently large distances between the atom and the surface, the interaction energy between the two is clearly

effected by the small values of the plasmon wave vectors. In this case, the effect of dispersion on the interaction energy is therefore not an important factor [6, 7] and hence is often neglected. When the distance between the atom and the surface is sufficiently small, the interaction energy is strongly influenced by large values of wave vectors. In this situation which is not studied well in earlier publications, the inclusion of dispersion is necessary and forms the main consideration of this thesis.

For our system, we consider a hydrogen atom placed at the center of a region between parallel surfaces formed by two semi-infinite metal slabs. The change in the energy of the hydrogen atom is calculated taking into account its interaction with the metal surfaces. The choice of our geometry is influenced by the experiments of Sandoghdar, Sukenik, Hinds and Horoché [8] who have observed experimentally, for the first time, the changes in the Rydberg energy states of a sodium atom when it is placed at the center of the gap. In this thesis, the unperturbed states of the hydrogen atom are taken to be their 1S, 3S, 10S and 14S states, the metal electrons are assumed to be in their ground state.

It is important to recognize that the plasmon modes in the two surfaces across the gap are strongly coupled to each other when the distance separating them is sufficiently small. This gives rise to two dispersed coupled plasmon modes which can be described as the symmetric and antisymmetric modes. If the width separating the metals is sufficiently large, the plasmon coupling is weak and consequently, the two coupled modes merge into a single

mode. If the bulk plasmon frequency is given by ω_p then the frequencies of the merged modes corresponds to $\omega_p/\sqrt{2}$ which is the well known expression for the surface plasmons for a single surface.

For widths much larger than the size of the atom, the dispersion effect will be shown to be small. In this case the interaction can be obtained with relative ease with the help of the dipolar approximation and the image theory of classical electrodynamics (which is independent of dispersion effects). The main assumption of the image theory is that all metals are considered to be a perfect conductors and therefore the self-energy obtained using the theory is independent of any other property of the metal. As the gap is reduced to about one or two nanometers, or even less as in the case of a hydrogen atom, the size of the atom becomes an important consideration in the calculation of the self-energy and the effect of dispersion becomes a significant factor. One of the important consequences of dispersion is that in the limit of the gap approaching zero the self-energy approaches a finite value while the self-energy obtained using the image theory diverges to infinity. The consideration of the plasmon dispersion also makes the self-energy dependent on the electron density of the metal. This result contrasts with the image theory result in which the self-energy does not change from one metal to another.

Although the self-energy of a charged particle, such as an electron or a positron placed between two metal slabs, has been obtained in earlier works [8, 9], the self energy of an atom

has not received the same attention. Recently [10], the self energy of an atom (neglecting dispersion effects) was evaluated using the same geometry as considered in this thesis. The present thesis, which includes the effect of dispersion, is a nontrivial generalization of the previous works [8] – [10]. In this thesis however, we have neglected the effect of the atomic motion in the interaction energy. The neglect is justifiable on the grounds that dynamical effects, being quantum in nature, are expected to be small for atoms which are considerably heavier than an electron or positron. We show in this thesis that when the gap is sufficiently small, the use of the image theory is inadequate and consideration of dispersion is essential. For example, in the earlier publication [10] in which the plasmon dispersion is neglected, the self-energy approaches infinity as the width is decreased. The present thesis shows that the consideration of dispersion leads to the saturation of the self-energy of the atom which is in sharp contrast to the result of the previous paper [10] .

The plan of the paper is as follows: In section 2, we treat the atom as a two body system and we express the Hamiltonian when the atom is placed between two metal plates. We make use of a unitary transformation, introduced earlier by Platzman [11], to express the interaction energy of the atom with the surfaces as a shift in the zero-point energy of the plasmon modes. In section 3 we obtain the individual values of the interaction energies of the electron and the nucleus. We also derive changes in the interaction energy between the electron and the nucleus in the presence of the two surfaces. The potential energy is obtained on the assumption that the nucleus is restricted to remain within the gap and

unable to penetrate the metal while the electron is allowed to exist anywhere in the entire system. In section 4, we assume that the nucleus of the hydrogen atom is within the gap and that the atom is in its ground state. We use the first order perturbation theory to obtain the effect of the interaction potential on the self-energy. We have obtained the self-energy of the atom considering the effects of the plasmon dispersion as well as the multipolar excitations of the atom. We have also extended the self-energy calculations to include the 3S, 10S and 14S excited states of the hydrogen atom. The calculations for the excited states, however, are approximate and are based on the dipolar assumption. Concluding remarks are given in section 5.

2 HAMILTONIAN

We express the Hamiltonian of our two particle system by generalizing the Hamiltonian developed earlier by Sols and Ritchie [9], for a charged particle within two parallel plates.

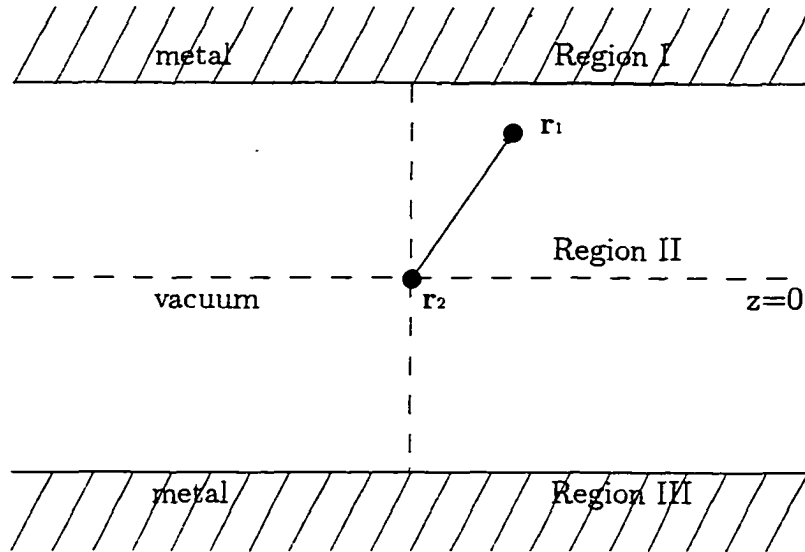


Figure 1. Two oppositely charged particles within two parallel plates.

Following the geometry in Figure 1, we write the Hamiltonian as

$$\widehat{H} = \frac{\mathbf{p}_n^2}{2m_n} + \frac{\mathbf{p}_e^2}{2m_e} - \frac{e^2}{|\mathbf{r}_1 - \mathbf{r}_2|} + \widehat{H}_{met} + \widehat{H}_{int}, \quad (1)$$

where the first two terms are the kinetic energies of the nucleus and electron respectively. m_n and m_e are the nucleus and electron masses, e is the absolute electron charge. \mathbf{r}_1 and \mathbf{r}_2 are the positional coordinates of the two oppositely charged particles. \widehat{H}_{met} is the Hamiltonian representing the metal electrons and \widehat{H}_{int} represents the interaction between the charged particles and the metal surfaces. We write the Hamiltonian for the metal in terms of the energy of the surface plasmons according to

$$\widehat{H}_{met} = \sum_{\mathbf{k}, \alpha} \hbar \omega_{\mathbf{k}, \alpha} \left[a_{\mathbf{k}, \alpha}^\dagger a_{\mathbf{k}, \alpha} + \frac{1}{2} \right]. \quad (2)$$

In eqn. (2), $a_{\mathbf{k}, \alpha}^\dagger$ and $a_{\mathbf{k}, \alpha}$ are respectively the creation and destruction operators for the surface plasmon modes denoted by a 2-dimensional wave vector \mathbf{k} and $\omega_{\mathbf{k}, \alpha}$ is the frequency of the plasmon mode for the wave vector \mathbf{k} . The quantity α takes values plus one for the symmetric mode and minus one for the anti-symmetric mode. In eqn. (2) we have neglected the effect of the bulk plasmons on the assumption that the effect of the surface plasmons are expected to dominate when the center of the atom is outside the metal. The interaction Hamiltonian for the two particles interacting with the metal surfaces is given by [9]

$$\widehat{H}_{int} = -e \sum_{\mathbf{k}, \alpha} \left[\Gamma_{\mathbf{k}, \alpha}(z_1) e^{i\mathbf{k} \cdot \mathbf{R}_1} - \Gamma_{\mathbf{k}, \alpha}(z_2) e^{i\mathbf{k} \cdot \mathbf{R}_2} \right] (a_{-\mathbf{k}, \alpha}^\dagger + a_{\mathbf{k}, \alpha}), \quad (3)$$

where $\Gamma_{k,\alpha}$ is the coupling constant and the electron position is denoted by cylindrical coordinates so that $\mathbf{r}_1 \equiv (\mathbf{R}_1, z_1)$ and the nuclear coordinate denoted by $\mathbf{r}_2 \equiv (\mathbf{R}_2, z_2)$. We choose the center of the gap as the origin of the z coordinate and restrict the nucleus to remain within the gap so that $-a < z_2 < a$ where the gap width $L = 2a$. The coupling constant $\Gamma_{k,\alpha}$ is given by [9]

$$\Gamma_{k,\alpha}(z) = g_{k,\alpha}^i(z) N_{k,\alpha} \quad (4)$$

where

$$N_{k,\alpha}^2 = \frac{\omega_p^2 (1 - \alpha e^{-2ka}) (2\omega_{k,\alpha}^2 - \omega_p^2 (1 + \alpha e^{-2ka}))^2 m \hbar}{32\pi^2 n e^2 k^3 A (\omega_{k,\alpha}^2 - \omega_p^2)^2 \omega_{k,\alpha} (3\omega_p^2 (1 - \alpha e^{-2ka}) + 2(\omega_{k,\alpha}^2 - \omega_p^2))}. \quad (5)$$

The dependence of $g_{k,\alpha}^i(z)$ on position $z = z_1$ for the electron and $z = z_2$ for the nucleus is defined by

$$\left. \begin{aligned} g_{k,\alpha}^1(z) &= \omega_{k,\alpha}^2 \gamma_{k,\alpha} e^{k(z+a)} - k\omega_p^2 e^{\gamma_{k,\alpha}(z+a)}, & z < -a \\ g_{k,\alpha}^2(z) &= \frac{(\omega_{k,\alpha}^2 \gamma_{k,\alpha} - k\omega_p^2)(e^{kz} + \alpha e^{-kz})}{(e^{ka} + \alpha e^{-ka})}, & -a < z < a \\ g_{k,\alpha}^3(z) &= \alpha (\omega_{k,\alpha}^2 \gamma_{k,\alpha} e^{k(-z+a)} - k\omega_p^2 e^{\gamma_{k,\alpha}(-z+a)}), & z > a. \end{aligned} \right\} \quad (6)$$

The dispersion of the surface plasmon frequency $\omega_{k,\alpha}$ derived earlier and discussed in Appendix A is expressed as

$$\omega_{k,\alpha}^2 = \frac{1}{2} \left(\omega_p^2 (1 + \alpha e^{-2ka}) + \beta^2 k^2 + \beta k (\beta^2 k^2 + 2\omega_p^2 (1 - \alpha e^{-2ka}))^{\frac{1}{2}} \right), \quad (7)$$

in which the dispersion parameter β has the value $\beta^2 = \frac{3}{5}v_f^2$ and v_f is the Fermi velocity of the electron gas. For all values of the dispersion parameter β , the surface plasmons frequency have two frequencies corresponding to the symmetric mode when $\alpha = +1$ and the antisymmetric mode when $\alpha = -1$. The parameter β is also related to γ which occurs in eqn. (6) by the relation

$$\gamma_{k,\alpha} = k^2 + \frac{(\omega_p^2 - \omega_{k,\alpha}^2)}{\beta^2}. \quad (8)$$

In the expression for the surface plasmon frequency given by eqn. (7), β is a convenient parameter to denote the dispersion effect due to the pressure exerted by the electron gas. The plasmon dispersion also arises due to the coupling of the plasmon modes in the two surfaces and is shown in Figure 2. When the gap width is large, the two coupled modes merge into a single frequency. At zero width, the antisymmetric mode has zero frequency and the symmetric mode has the frequency corresponding to bulk plasmons. Although we

consider both of the dispersions, for the purpose of this thesis we refer to the dispersion as the one induced by the pressure of the electron fluid and not the one dependent on the gap width.

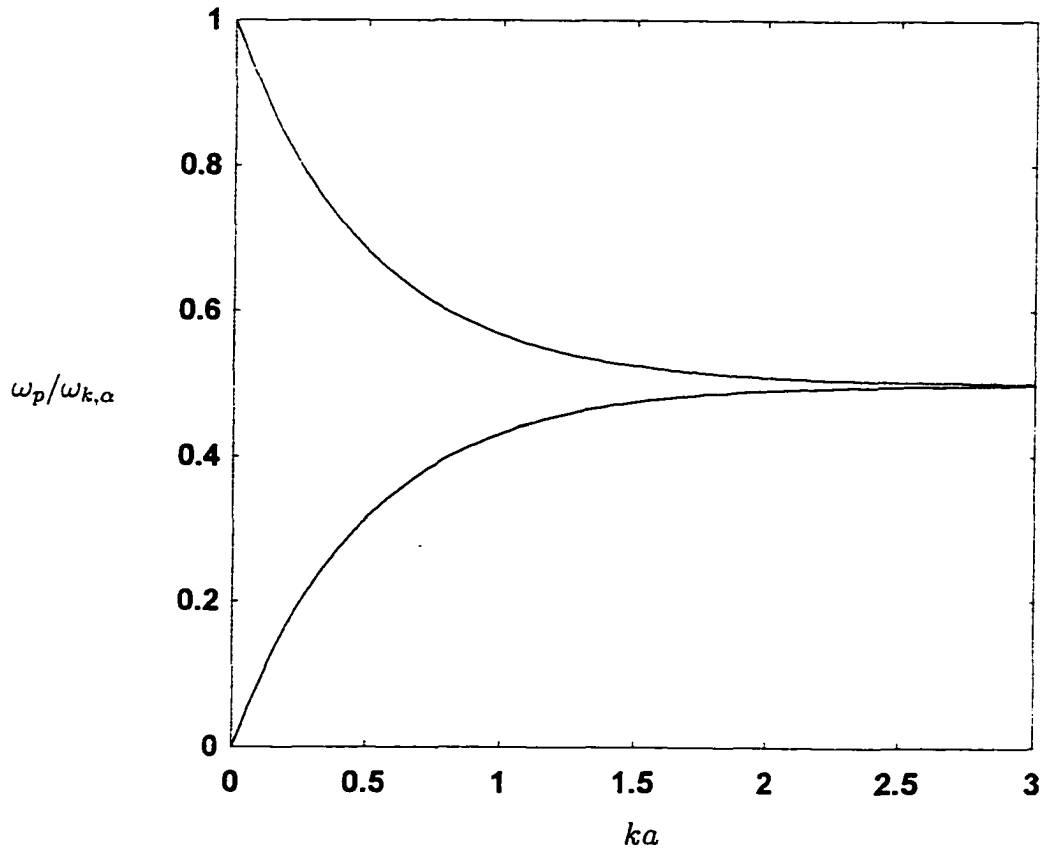


Figure 2. $\frac{\omega_p}{\omega_{k,\alpha}}$ as a function of ka

We now rewrite the Hamiltonian by using a unitary transformation which allows us to express the interaction energy as a shift in the zero-point energy of the surface plasmon modes. The unitary transformation \hat{U} is similar to the one used by Platzman [11] in the polaron theory. It can be defined by

$$\hat{U} = \exp \sum_{\mathbf{k}, \alpha} \left(f_{\mathbf{k}, \alpha} a_{\mathbf{k}, \alpha} - f_{\mathbf{k}, \alpha}^* a_{\mathbf{k}, \alpha}^\dagger \right). \quad (9)$$

The operator $a_{\mathbf{k}, \alpha}$ transforms accordingly as

$$\hat{U}^{-1} a_{\mathbf{k}, \alpha} \hat{U} = a_{\mathbf{k}, \alpha} + f_{\mathbf{k}, \alpha}, \quad (10)$$

where the parameter $f_{\mathbf{k}, \alpha}$ is ascribed a value such that the linear terms in $a_{-\mathbf{k}, \alpha}$ and $a_{\mathbf{k}, \alpha}$ in the transformed Hamiltonian

$$\hat{H}_t = \hat{U}^{-1} \hat{H} \hat{U}, \quad (11)$$

are eliminated. The value of $f_{\mathbf{k}, \alpha}$ which achieves this elimination is given by

$$\begin{aligned} f_{\mathbf{k}, \alpha} &= f_{\mathbf{k}, \alpha}(z_1, z_2, \mathbf{R}) \\ &= \frac{q}{\hbar \omega_{\mathbf{k}, \alpha}} \left[e^{-i\mathbf{k} \cdot \mathbf{R}_1} \Gamma_{\mathbf{k}, \alpha}(z_1) - \Gamma_{\mathbf{k}, \alpha}(z_2) e^{-i\mathbf{k} \cdot \mathbf{R}_2} \right]. \end{aligned} \quad (12)$$

If we neglect the effect of the unitary transformation on the momentum operators in eqn.

(1) then the transformed Hamiltonian is expressed by

$$\widehat{H}_t = \frac{\mathbf{p}_n^2}{2m_n} + \frac{\mathbf{p}_e^2}{2m_e} - \frac{e^2}{|\mathbf{r}_1 - \mathbf{r}_2|} + \sum_{\mathbf{k}, \alpha} \hbar\omega \left[a_{\mathbf{k}, \alpha}^\dagger a_{\mathbf{k}, \alpha} + f_{\mathbf{k}, \alpha} f_{\mathbf{k}, \alpha}^* + \frac{1}{2} \right]. \quad (13)$$

In neglecting the effect of the transformation on the momentum operators, we have effectively neglected the consequence of the motion of the atom on the atom-surface interaction. Substituting the expression for $f_{\mathbf{k}, \alpha}$ into (13), we are able to write the potential energy according to

$$V = \frac{-e^2}{|\mathbf{r}_1 - \mathbf{r}_2|} + \Delta V, \quad (14)$$

where the first term is the bare coulomb energy between the two charges and ΔV is a result of the interaction of the charges with the two surfaces. The shift ΔV in the potential energy of the atom is given by

$$\Delta V = V_1(z_1) + V_2(z_2) + V_3(z_1, z_2; \mathbf{R}) \quad (15)$$

where $\mathbf{R} = \mathbf{R}_1 - \mathbf{R}_2$. The transformed Hamiltonian can now be expressed as

$$\begin{aligned} \widehat{H}_t = & \frac{p_n^2}{2m_n} + \frac{p_e^2}{2m_e} - \frac{e^2}{|\mathbf{r}_1 - \mathbf{r}_2|} + \sum_{\mathbf{k}, \alpha} \hbar\omega \left[a_{\mathbf{k}, \alpha}^\dagger a_{\mathbf{k}, \alpha} + \frac{1}{2} \right] \\ & + V_1(z_1) + V_2(z_2) + V_3(z_1, z_2, \mathbf{R}) \end{aligned} \quad (16)$$

where

$$V_1(z_1) = -e^2 \sum_{\mathbf{k}, \alpha} \frac{|\Gamma_{\mathbf{k}, \alpha}(z_1)|^2}{\hbar \omega_{\mathbf{k}, \alpha}} \quad (17)$$

is the self energy of the electron interacting with the metal surfaces,

$$V_2(z_2) = -e^2 \sum_{\mathbf{k}, \alpha} \frac{|\Gamma_{\mathbf{k}, \alpha}(z_2)|^2}{\hbar \omega_{\mathbf{k}, \alpha}} \quad (18)$$

is the self energy of the nucleus and

$$V_3(z_1, z_2, \mathbf{R}) = 2e^2 \sum_{\mathbf{k}, \alpha} \frac{e^{i\mathbf{k} \cdot \mathbf{R}} \Gamma_{\mathbf{k}, \alpha}(z_1) \Gamma_{\mathbf{k}, \alpha}(z_2)}{\hbar \omega_{\mathbf{k}, \alpha}} \quad (19)$$

is the change in the interaction energy between the electron and the nucleus arising from its interaction with the surfaces.

3 POTENTIAL ENERGIES

If we now substitute eqns. (4) to (6) into eqn. (15) to write the potential energy of the electron in the presence of the two surfaces. The functional dependence of the potential energy $V_1(z_1)$ on the position of the electron in the three regions as denoted in Figure 1, is given by the expression

$$V_1(z_1) = -e^2 \sum_{\mathbf{k}, \alpha} \int \frac{2\pi}{\hbar\omega_{\mathbf{k}, \alpha}} N_{\mathbf{k}, \alpha}^2 k dk \times \quad (20)$$

$$\left[\left\{ g_{\mathbf{k}, \alpha}^1(z_1) \right\}^2 \Theta(-z_1 - a) + \left\{ g_{\mathbf{k}, \alpha}^2(z_1) \right\}^2 \Theta(z_1 + a) \Theta(a - z_1) + \left\{ g_{\mathbf{k}, \alpha}^3(z_1) \right\}^2 \Theta(z_1 - a) \right]$$

where $\Theta(z) = 1$ for $z > 0$ and $\Theta(z) = 0$ for $z < 0$ which allows us to express $V(z)$, (which has different values in the three regions), by a single expression. The potential energy $V_2(z_2)$ of the nucleus can also be written in the same way as the expression for $V_1(z_1)$ except that the nucleus is now restricted to region II, by our choice.

$$V_2(z_2) = -e^2 \sum_{\mathbf{k}, \alpha} \int \frac{2\pi}{\hbar\omega_{\mathbf{k}, \alpha}} N_{\mathbf{k}, \alpha}^2 k dk \times \left[\left\{ g_{\mathbf{k}, \alpha}^2(z_2) \right\}^2 \Theta(z_2 + a) \Theta(a - z_2) \right]. \quad (21)$$

The change in the interaction energy $V_3(z_1, z_2, R)$ between the electron and the nucleus is

given by

$$V_3(z_1, z_2, R) = 2e^2 \sum_{k,\alpha} \int J_o(kR) \frac{2\pi}{\hbar\omega_{k,\alpha}} N_{k,\alpha}^2 k dk \times g_{k,\alpha}^2(z_2) \Theta(z_2 + a) \Theta(a - z_2) \times \quad (22)$$

$$\left[g_{k,\alpha}^1(z_1) \Theta(-z_1 - a) + g_{k,\alpha}^2(z_1) \Theta(z_1 + a) \Theta(a - z_1) + g_{k,\alpha}^3(z_1) \Theta(z_1 - a) \right].$$

If we substitute values of $g_{k,\alpha}^i$ from eqns. (6) into eqns. (20) to (22), we immediately conclude that $V_1(z_1)$ and $V_3(z_1, z_2, R)$ are continuous for all values of z_1 , in particular at the boundary $z_1 = \pm a$, and for a specified value of z_2 within the gap. The following summarizes the potential energies for all three regions.

REGION I ($z_1 < -a$, $-a < z_2 < a$)

$$V_1(z_1) = -e^2 \int_0^\infty dk \frac{(\omega_{k\pm}^2 \gamma_{k\pm} e^{k(z_1+a)} - k\omega_p^2 e^{\gamma_{k\pm}(z_1+a)})^2}{4k^2 (\omega_{k\pm}^2 - \omega_p^2)^2}$$

$$\times \frac{(1 \mp e^{-2ka}) (2\omega_{k\pm}^2 - \omega_p^2 (1 \pm e^{-2ka}))^2}{\omega_{k\pm}^2 (3\omega_p^2 (1 \mp e^{-2ka}) + 2(\omega_{k\pm}^2 - \omega_p^2))} \quad (23)$$

$$V_3(z_1, z_2, R) = 2e^2 \int_0^\infty dk \frac{J_o(kR) (1 \mp e^{-2ka}) (\omega_{k\pm}^2 \gamma_{k\pm} e^{k(z_1+a)} - k\omega_p^2 e^{\gamma_{k\pm}(z_1+a)})}{4k^2 (\omega_{k\pm}^2 - \omega_p^2)^2}$$

$$\times \frac{(\omega_{k\pm}^2 \gamma_{k\pm} - k\omega_p^2) (2\omega_{k\pm}^2 - \omega_p^2 (1 \pm e^{-2ka}))^2 (e^{-kz_2} \pm e^{kz_2})}{\omega_{k\pm}^2 (3\omega_p^2 (1 \mp e^{-2ka}) + 2(\omega_{k\pm}^2 - \omega_p^2)) (e^{ka} \pm e^{-ka})} \quad (24)$$

REGION II $(-a < z_1 < a, -a < z_2 < a)$

$$V_1(z_1) = -e^2 \int_0^\infty dk \frac{(1 \mp e^{-2ka}) (2\omega_{k\pm}^2 - \omega_p^2 (1 \pm e^{-2ka}))^2}{4k^2 (\omega_{k\pm}^2 - \omega_p^2)^2} \\ \times \frac{(\omega_{k\pm}^2 \gamma_{k\pm} - k\omega_p^2)^2 (e^{-kz_1} \pm e^{kz_1})^2}{\omega_{k\pm}^2 (3\omega_p^2 (1 \mp e^{-2ka}) + 2(\omega_{k\pm}^2 - \omega_p^2)) (e^{ka} \pm e^{-ka})^2} \quad (25)$$

$$V_2(z_2) = -e^2 \int_0^\infty dk \frac{(1 \mp e^{-2ka}) (2\omega_{k\pm}^2 - \omega_p^2 (1 \pm e^{-2ka}))^2}{4k^2 (\omega_{k\pm}^2 - \omega_p^2)^2} \\ \times \frac{(\omega_{k\pm}^2 \gamma_{k\pm} - k\omega_p^2)^2 (e^{-kz_2} \pm e^{kz_2})^2}{\omega_{k\pm}^2 (3\omega_p^2 (1 \mp e^{-2ka}) + 2(\omega_{k\pm}^2 - \omega_p^2)) (e^{ka} \pm e^{-ka})^2} \quad (26)$$

$$V_3(z_1, z_2, R) = 2e^2 \int_0^\infty dk \frac{J_0(kR) (1 \mp e^{-2ka}) (2\omega_{k\pm}^2 - \omega_p^2 (1 \pm e^{-2ka}))^2}{4k^2 (\omega_{k\pm}^2 - \omega_p^2)^2} \\ \times \frac{(\omega_{k\pm}^2 \gamma_{k\pm} - k\omega_p^2)^2 (e^{kz_1} \pm e^{-kz_1}) (e^{-kz_2} \pm e^{kz_2})}{\omega_{k\pm}^2 (3\omega_p^2 (1 \mp e^{-2ka}) + 2(\omega_{k\pm}^2 - \omega_p^2)) (e^{ka} \pm e^{-ka})^2} \quad (27)$$

REGION III ($z_1 > a, -a < z_2 < a$)

$$V_1(z_1) = -e^2 \int_0^\infty dk \frac{(1 \mp e^{-2ka}) (2\omega_{k\pm}^2 - \omega_p^2 (1 \pm e^{-2ka}))^2}{4k^2 (\omega_{k\pm}^2 - \omega_p^2)^2} \times \frac{(\omega_{k\pm}^2 \gamma_{k\pm} e^{-k(z_1-a)} - k\omega_p^2 e^{-\gamma_{k\pm}(z_1-a)})^2}{\omega_{k\pm}^2 (3\omega_p^2 (1 \mp e^{-2ka}) + 2(\omega_{k\pm}^2 - \omega_p^2))} \quad (28)$$

$$V_3(z_1, z_2, R) = 2e^2 \int_0^\infty dk \frac{J_0(kR) (1 \mp e^{-2ka}) (2\omega_{k\pm}^2 - \omega_p^2 (1 \pm e^{-2ka}))^2}{4k^2 (\omega_{k\pm}^2 - \omega_p^2)^2} \times \frac{(\pm) (\omega_{k\pm}^2 \gamma_{k\pm} e^{-k(z_1-a)} - k\omega_p^2 e^{-\gamma_{k\pm}(z_1-a)}) (\omega_{k\pm}^2 \gamma_{k\pm} - k\omega_p^2) (e^{-kz_2} \pm e^{kz_2})}{\omega_{k\pm}^2 (3\omega_p^2 (1 \mp e^{-2ka}) + 2(\omega_{k\pm}^2 - \omega_p^2)) (e^{ka} \pm e^{-ka})} \quad (29)$$

When the dispersion effects are neglected, the potential energy is given by the theory of images. To show this result, we combine eqns. (7) and (8) to obtain the following relations,

$$\gamma_{k\alpha} = \frac{k\omega_p^2 (1 - \alpha e^{-2ka})}{[2\omega_{k,\alpha}^2 - \omega_p^2 (1 + \alpha e^{-2ka})]} \quad (30)$$

and

$$\omega_{k,\alpha}^2 - \omega_p^2 = -\omega_p^2 (1 - \alpha e^{-2ka}) / 2. \quad (31)$$

Substituting eqns. (30) and (31) into (21) and changing the summation to integration, the potential energy $V_1(z_1)$ of the electron within the gap, is given by

$$V_1(z_1) = -\frac{e^2}{8a} \left[2\Phi\{1\} - \Phi\left\{\frac{1}{2} + \frac{z_1}{2a}\right\} - \Phi\left\{\frac{1}{2} - \frac{z_1}{2a}\right\} \right] \quad (32)$$

where

$$\Phi(y) = -\int_0^\infty \frac{e^{-yt}}{1 - e^{-t}} dt. \quad (33)$$

The potential energy of a single particle in the gap given by eqn. (32) exactly corresponds to the expression obtained by Sols and Ritchie [9]. Moreover, this result is the same if we had used the classical image theory.

3.1 Results

We have numerically evaluated the potentials $V(z_1)$, $V(z_2)$ and $V(z_1, z_2, R)$ from eqns. (20) to (22). In Figures 3 - 5 we show the effect of dispersion on the potential energies of a electron and a electron-nucleus pair placed within a gap between two metal surfaces. We observe

that the potential energy is weakened for both of the cases as a result of the dispersion. Furthermore, the potential is observed to saturate to a finite value in the presence of the dispersion, while it diverges at the surface in its absence.

In Figure 3, the variation in the potential energy, in units of e^2/a , is shown by the dashed line for an electron as a function of the distance measured from the center of the gap, in units of a , in the absence of dispersion. As expected the potential energy at the center of the gap has the value $\frac{\ln 2}{2}$ as given by equation (32). The potential energy close to the surface varies with z as $\frac{1}{z-a}$ and this behavior is clearly seen in Figure 3. Outside of the gap, the potential is symmetric with respect to the origin but is not symmetric with respect to the surface.

Also in Figure 3, the potential energy of a particle is shown for the three following values of r_s of the metal electrons representing Be ($r_s = 1.88$), Ag ($r_s = 3.02$) and Cs ($r_s = 5.63$). The dispersive effects defined by eqn. (7) are observed to be strong for small r_s . The potential at the center is considerably screened while at the surface it approaches a finite value. The saturated value is largely negative when r_s is small.

In Figure 4, the variation in the potential energy of the electron as a function of z_1 is shown when the nucleus is located at the center of the gap with the horizontal distance R between the two particles is set to zero. Figure 4 shows the variation when dispersion is neglected (dashed curve), as well as the potential energy with dispersion effects included for the three values of r_s .

Figures 5 shows the variation of the change in potential energy due to the surface as a

function of R from the image theory and for the three previous values for r_s with dispersion included. Clearly, the energy decreases as R increases but saturates to a value $\ln 2$ as expected from the image theory.

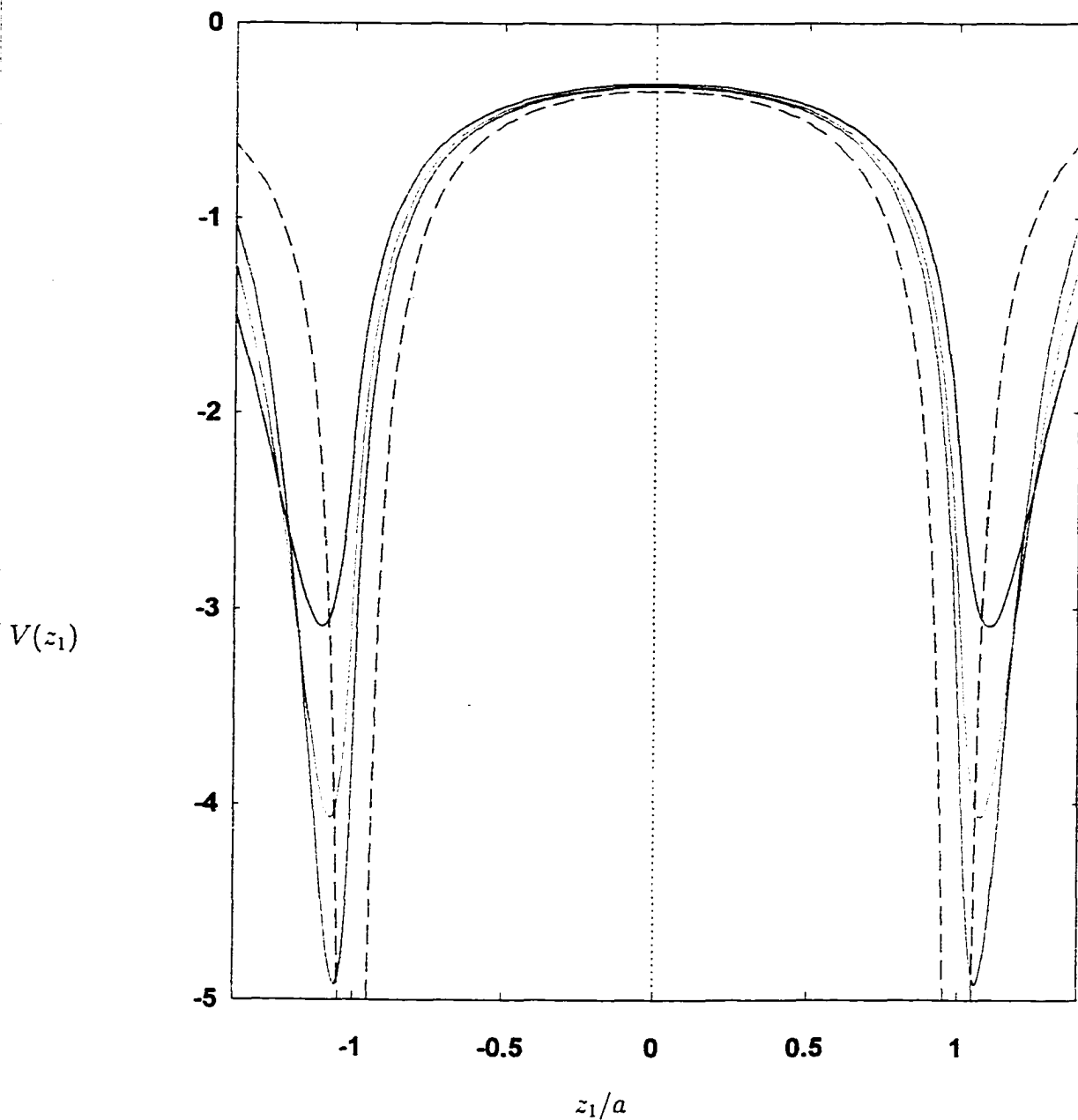


Figure 3. Potential energy of an electron (in units of $\frac{e^2}{a}$) as a function of its position z_1 with a gap width of $L = 2a$ where $a = 1.0 \times 10^{-7} \text{cm}$. The red, green and blue curves are for $r_s = 1.88$, $r_s = 3.02$ and $r_s = 5.63$ respectively. The dashed curve represents the image potential (dispersionless).

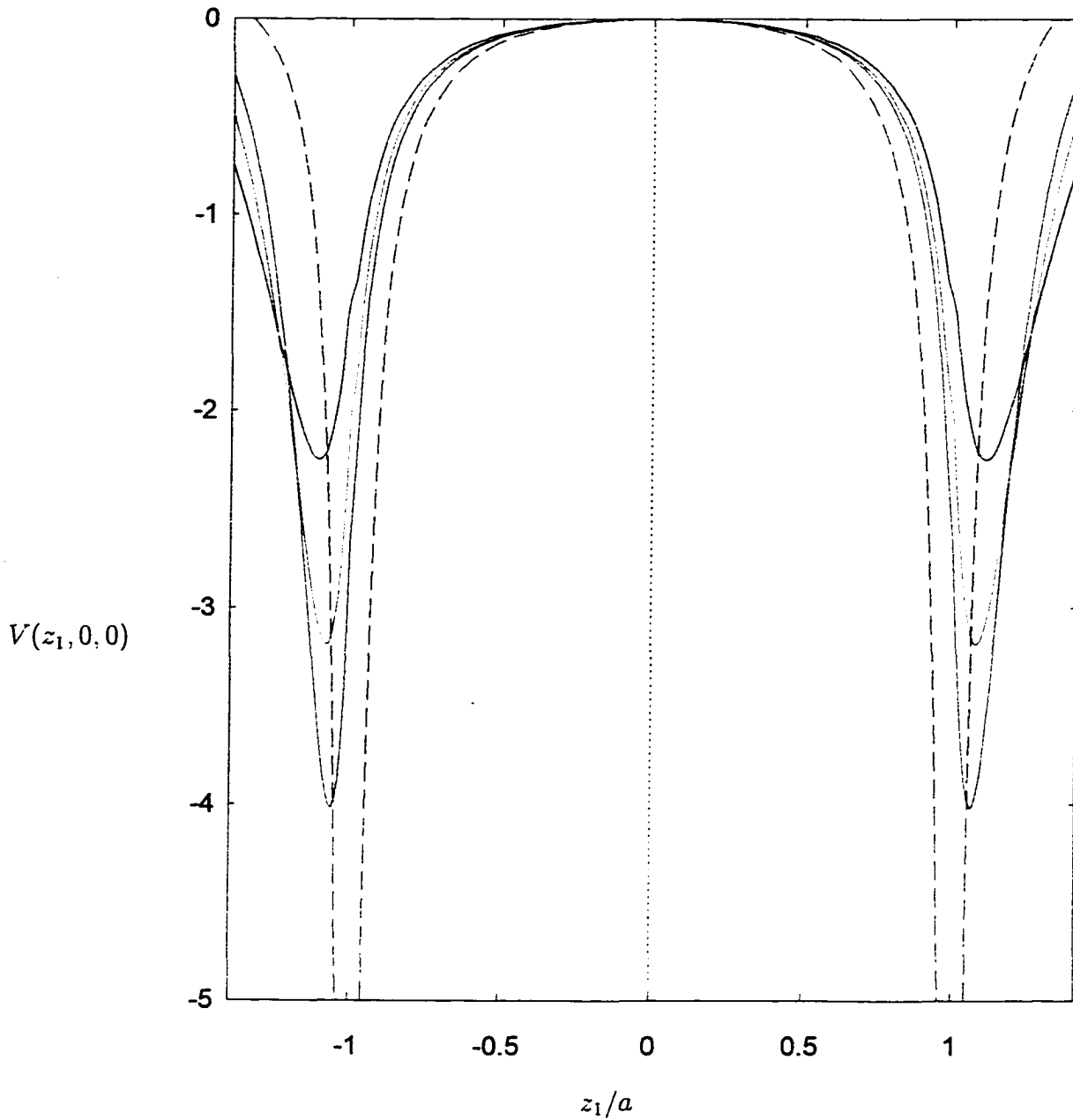


Figure 4. Potential energy of an atom (in units of $\frac{e^2}{a}$) as a function of its position z_1 . The nucleus is set at $z_2 = 0$ and the gap width is $L = 2a$ where $a = 1.0 \times 10^{-7} \text{ cm}$. The red, green and blue curves are for $r_s = 1.88$, $r_s = 3.02$ and $r_s = 5.63$ respectively. The dashed curve represents the image potential (dispersionless).

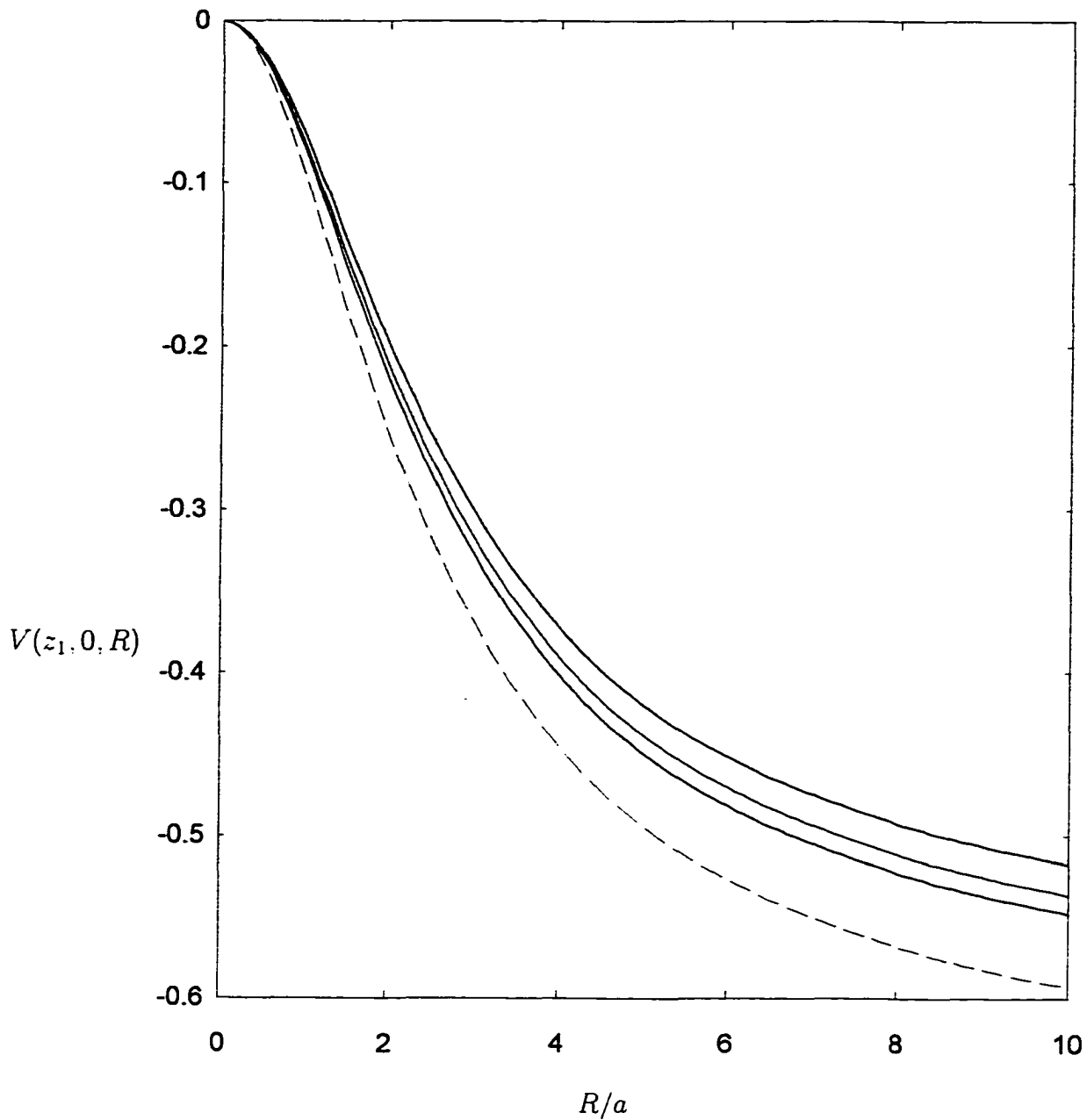


Figure 5. Potential energy of an atom (in units of $\frac{e^2}{a}$) as a function of the horizontal distance between the electron and the nucleus with a gap width of $L = 2a$ where $a = 1.0 * 10^{-7} \text{cm}$. The red, green and blue curves are for $r_s = 1.88$, $r_s = 3.02$ and $r_s = 5.63$ respectively. The dashed curve represents the image potential (dispersionless).

4 ENERGY STATES OF A HYDROGEN ATOM

4.1 Ground State

We now treat the interaction energy of the electron due to the surfaces as a perturbation to obtain the first order change in the ground state energy of the hydrogen atom. Let the ground state wave function of the hydrogen atom be given by

$$\psi_0(z, R) = \frac{1}{\pi^{1/2} a_0^{3/2}} \exp\left(-\frac{1}{a_0} \sqrt{R^2 + z^2}\right) \quad (34)$$

where a_0 is the Bohr radius. The relative coordinate z of the electron with respect to the nucleus is defined by $z = z_1 - z_2$ and similarly $R = R_1 - R_2$. For simplicity we set $z_2 = 0$ so that the nucleus is at the center of the gap. Using the unperturbed wave function of the hydrogen atom given above, we express the change in its energy ΔE due to the perturbation potential according to

$$\Delta E = E_1(z_1) + E_2(z_2) + E_3(z_1, z_2, R) \quad (35)$$

where $E_2(z_2)$ is the potential energy of the nucleus anchored at z_2 ,

$$E_1(z_1) = -e^2 \sum_{k,\alpha} \int \frac{2\pi}{\hbar\omega_{k,\alpha}} N_{k,\alpha}^2 k dk \times \quad (36)$$

$$\left[\langle \{g_{k,\alpha}^1(z_1)\}^2 \Theta(-z_1 - a) + \{g_{k,\alpha}^2(z_1)\}^2 \Theta(z_1 + a) \Theta(a - z_1) + \{g_{k,\alpha}^3(z_1)\}^2 \Theta(z_1 - a) \rangle \right]$$

and

$$E_3(z_1, z_2, R) = 2e^2 \sum_{k,\alpha} \int \frac{2\pi}{\hbar\omega_{k,\alpha}} N_{k,\alpha}^2 k dk \times g_{k,\alpha}^2(z_2) \Theta(z_2 + a) \Theta(a - z_2) \times \quad (37)$$

$$\left[\langle J_o(kR) \{g_{k,\alpha}^1(z_1) \Theta(-z_1 - a) + g_{k,\alpha}^2(z_1) \Theta(z_1 + a) \Theta(a - z_1) + g_{k,\alpha}^3(z_1) \Theta(z_1 - a)\} \rangle \right]$$

The averaging $\langle f(z, R) \rangle$ over the wave function is defined as

$$\langle f(z, R) \rangle = \int_{-\infty}^{\infty} \int_0^{\infty} f(z, R) \psi_o^*(z, R) \psi_o(z, R) R dR dz. \quad (38)$$

All the integrals using averaging process defined by eqn. (38) can be done by analytical methods and are given in the Appendix B. Hence the change in the energy ΔE in eqn. (35) can be realized by numerical integration over k . The succeeding summarizes the interaction energies for all three regions where $I_1, I_{2\pm}, I_{3\pm}, J_1, J_{2\pm}, K_1, K_2, K_3, L_1, L_2, M_1, M_{2\pm}, M_{3\pm}, N_1, N_{2\pm}$ and $N_{3\pm}$ are the integral defined by eqn. (38).

REGION I

$$E_1(z_1) = -\frac{2e^2}{a_0^3} \int dk \frac{(\omega_{k\pm}^4 \gamma_{k\pm}^2 I_1 - 2\omega_{\pm}^2 k \gamma_{\pm} I_{2\pm} + k^2 \omega_p^4 I_{3\pm})}{4k^2 (\omega_{k\pm}^2 - \omega_p^2)^2} \times \frac{(1 \mp e^{-2ka}) (2\omega_{k\pm}^2 - \omega_p^2 (1 \pm e^{-2ka}))^2}{\omega_{k\pm}^2 (3\omega_p^2 (1 \mp e^{-2ka}) + 2 (\omega_{k\pm}^2 - \omega_p^2))} \quad (39)$$

$$E_3(z_1, z_2, R) = \frac{4e^2}{a_0^3} \int dk \frac{J_0(k \cdot R) (\omega_{k\pm}^2 \gamma_{k\pm} J_1 - k \omega_p^2 J_{2\pm}) (1 \mp e^{-2ka})}{4k^2 (\omega_{k\pm}^2 - \omega_p^2)^2} \times \frac{(2\omega_{k\pm}^2 - \omega_p^2 (1 \pm e^{-2ka}))^2 (\omega_{k\pm}^2 \gamma_{k\pm} - k \omega_p^2) (e^{-kz_2} \pm e^{kz_2})}{\omega_{k\pm}^2 (3\omega_p^2 (1 \mp e^{-2ka}) + 2 (\omega_{k\pm}^2 - \omega_p^2)) (e^{ka} \pm e^{-ka})} \quad (40)$$

REGION II

$$E_1(z_1) = -e^2 \int dk \frac{(1 \mp e^{-2ka}) (2\omega_{k\pm}^2 - \omega_p^2 (1 \pm e^{-2ka}))^2}{4k^2 (\omega_{k\pm}^2 - \omega_p^2)^2} \times \frac{(\omega_{k\pm}^2 \gamma_{k\pm} - k \omega_p^2) (K_1 + K_2 \pm 2K_3)}{\omega_{k\pm}^2 (3\omega_p^2 (1 \mp e^{-2ka}) + 2 (\omega_{k\pm}^2 - \omega_p^2)) (e^{ka} \pm e^{-ka})^2} \quad (41)$$

$$\begin{aligned}
E_2(z_2) = & -e^2 \int dk \frac{(1 \mp e^{-2ka}) (2\omega_{k\pm}^2 - \omega_p^2 (1 \pm e^{-2ka}))^2}{4k^2 (\omega_{k\pm}^2 - \omega_p^2)^2} \\
& \times \frac{(\omega_{k\pm}^2 \gamma_{k\pm} - k\omega_p^2) (e^{-kz_2} \pm e^{kz_2})^2}{\omega_{k\pm}^2 (3\omega_p^2 (1 \mp e^{-2ka}) + 2(\omega_{k\pm}^2 - \omega_p^2)) (e^{ka} \pm e^{-ka})^2}
\end{aligned} \tag{42}$$

$$\begin{aligned}
E_3(z_1, z_2, R) = & 2e^2 \int dk \frac{J_0(kR) (1 \mp e^{-2ka}) (2\omega_{k\pm}^2 - \omega_p^2 (1 \pm e^{-2ka}))^2}{4k^2 (\omega_{k\pm}^2 - \omega_p^2)^2} \\
& \times \frac{(\omega_{k\pm}^2 \gamma_{k\pm} - k\omega_p^2) (L_1 \pm L_2) (e^{-kz_2} \pm e^{kz_2})}{\omega_{k\pm}^2 (3\omega_p^2 (1 \mp e^{-2ka}) + 2(\omega_{k\pm}^2 - \omega_p^2)) (e^{ka} \pm e^{-ka})^2}
\end{aligned} \tag{43}$$

REGION III

$$\begin{aligned}
E_1(z_1) = & -e^2 \int dk \frac{(\omega_{k\pm}^4 \gamma_{k\pm}^2 M_1 - 2\omega_{k\pm}^2 k \gamma_{k\pm} M_2 \pm k^2 \omega_p^4 M_3 \pm)}{4k^2 (\omega_{k\pm}^2 - \omega_p^2)^2} \\
& \times \frac{(1 \mp e^{-2ka}) (2\omega_{k\pm}^2 - \omega_p^2 (1 \pm e^{-2ka}))^2}{\omega_{k\pm}^2 (3\omega_p^2 (1 \mp e^{-2ka}) + 2(\omega_{k\pm}^2 - \omega_p^2))}
\end{aligned} \tag{44}$$

$$\begin{aligned}
E_3(z_1, z_2, R) = & 2e^2 \int dk \frac{J_0(kR) (1 \mp e^{-2ka}) (2\omega_{k\pm}^2 - \omega_p^2 (1 \pm e^{-2ka}))^2}{4k^2 (\omega_{k\pm}^2 - \omega_p^2)^2} \\
& \times \frac{(\pm) (\omega_{k\pm}^2 \gamma_{k\pm} N_1 - k\omega_p^2 N_{2\pm}) (\omega_{k\pm}^2 \gamma_{k\pm} - k\omega_p^2) (e^{-kz_2} \pm e^{kz_2})}{\omega_{k\pm}^2 (3\omega_p^2 (1 \mp e^{-2ka}) + 2 (\omega_{k\pm}^2 - \omega_p^2)) (e^{ka} \pm e^{-ka})}
\end{aligned} \tag{45}$$

4.2 The 3S, 10S and 14S Excited States

We know use the dipolar approximation to obtain the self-energies of the 3S, 10S and 14S excited states of a hydrogen atom placed within the gap with the nucleus set at the origin. Here, eqns. (21) to (23) are expanded up to the quadratic terms in z and R . The self-energy for the n th radial quantum state of the atom is given by

$$\Delta E_n = \langle n | V(z_1, z_2, \mathbf{R}) | n \rangle. \tag{46}$$

Equation (46) may be generalized to other hydrogenic atoms by replacing n with $n^* = (n - \delta)$ to account for the quantum defect. For hydrogen $\delta = 0$ while for sodium, $\delta \approx 1.3$.

4.3 Results

The value of ΔE is obtained numerically for the ground state of the hydrogen atom when $z_2 = 0$ when gap is altered from $L = 0$ to $L \approx 20a_0$, and the changes in ΔE are plotted. The numerical results are obtained for various values of r_s and for comparison, we have plotted ΔE when the dispersion is removed.

In Figure 6, the dashed line gives the variation in ΔE for the 1S state of the hydrogen atom as the gap is changed and the dispersion effects are neglected. We observe that the energy diverges as a approaches zero. This is expected since the potential is shown to diverge at the surface in this case, while in the presence of dispersion ΔE approaches a finite value. These however, depend on r_s and hence the metal. The dispersion in all cases, tend to screen the potential energy and the value of ΔE , although negative, increases from its dispersionless case.

In Figure 7, we have plotted the change in energy as the position of the hydrogen atom when z_2/a is altered from $z_2/a = 0$ to $z_2/a = 1$. The energy decreases initially as the atom approaches the surface and attains a minimum value before rising at the surface. We notice the binding to be large as r_s decreases. This result could be tested experimentally. Such an experiment would give credibility to the conclusion regarding the dispersion effect on ΔE as presented in this thesis.

In Figures 8 - 10, the dipolar approximation is used to show the variation of ΔE of the hydrogen atom as the gap is varied for the 3S, 10S and 14S states respectively. As is the case for the 1S state, we observe that the effect of dispersion on ΔE to be strong as the gap is decreased. In Figures 8 - 10, we notice the effects of dispersion for the values of r_s to be significant when the gap width is $20a_o$ (3S state), $70a_o$ (10S state) and $100a_o$ (14S state). It should be noted that the validity of ΔE for gap widths smaller than the widths stated above for the nS states should be considered uncertain and strongly questionable. The calculations were carried out using Monte Carlo integration and became increasingly sporadic for gap widths smaller than those stated. Also, since the potential energy (Figure 4) is highly peaked when the atom is close to the surface, the use of first order perturbation theory is questionable for gap widths smaller than $20a_o$, $70a_o$ and $100a_o$ for the 3S, 10S and 14S states respectively.

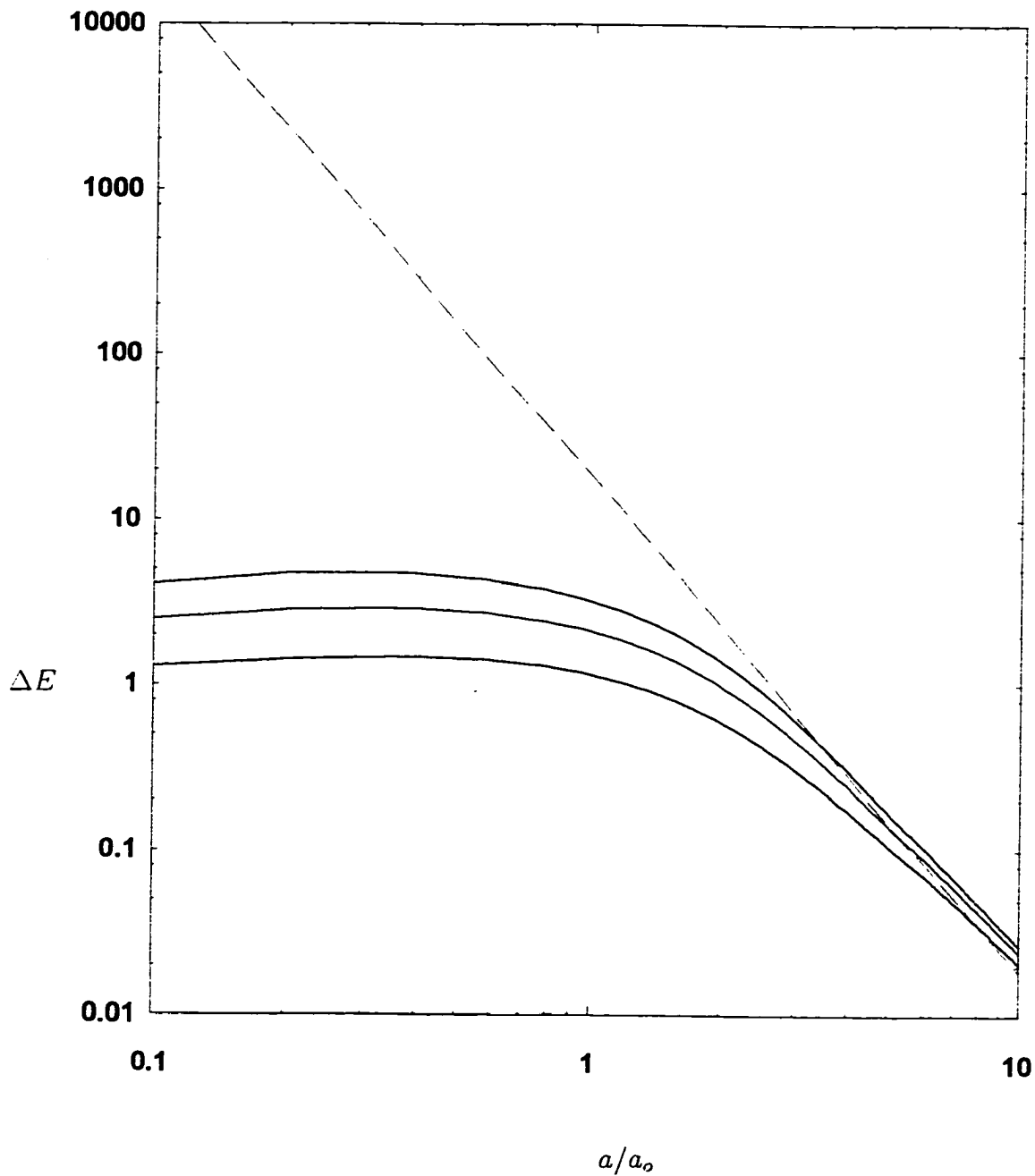


Figure 6. Self-energy (in eV) of a hydrogen atom as a function of the gap with the nucleus set at $z_2 = 0$. The red, green and blue curves are for $r_s = 1.88$, $r_s = 3.02$ and $r_s = 5.63$ respectively.

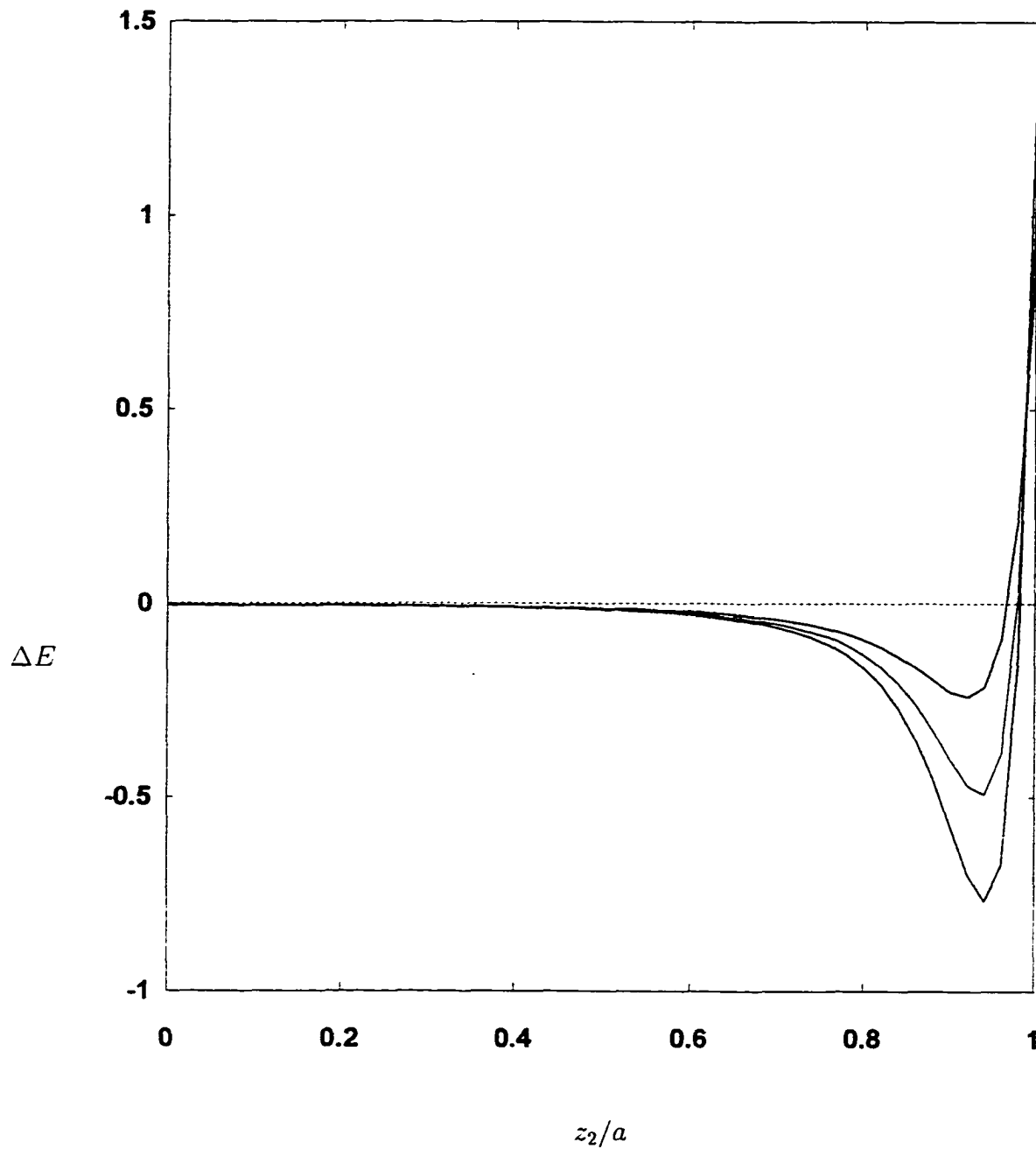


Figure 7. Self-energy of a hydrogen atom (in eV) as a function of the nucleus position z_2 .

The gap width is $L = 2a$ where $a = 1.0 \times 10^{-7} \text{ cm}$. The red, green and blue curves are for $r_s = 1.88$, $r_s = 3.02$ and $r_s = 5.63$ respectively.

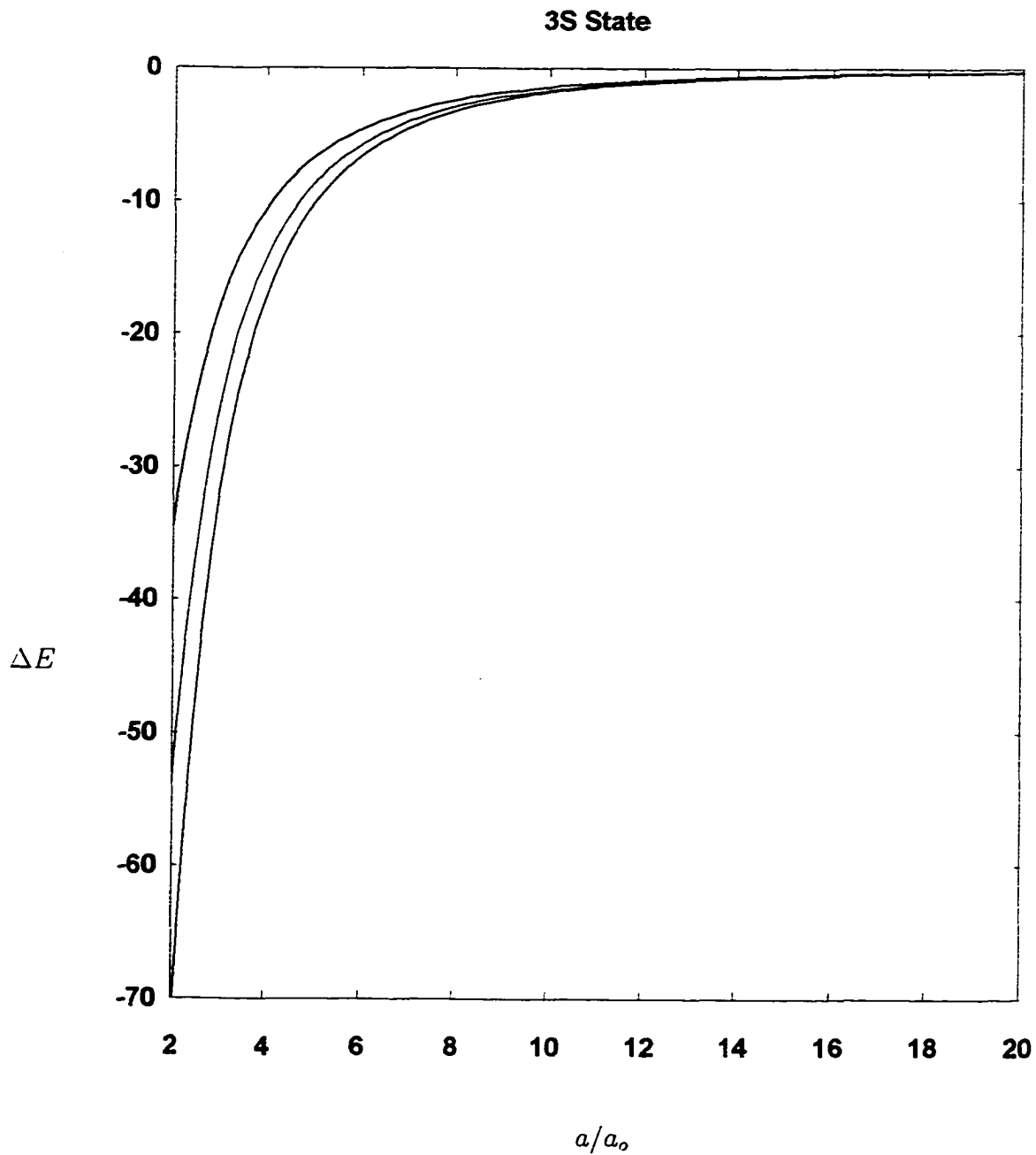


Figure 8. Self-energy (in eV) of a hydrogen atom, in the 3S excited state, as a function of the gap with the nucleus set at $z_2 = 0$. The red, green and blue curves are for $r_s = 1.88$, $r_s = 3.02$ and $r_s = 5.63$ respectively.

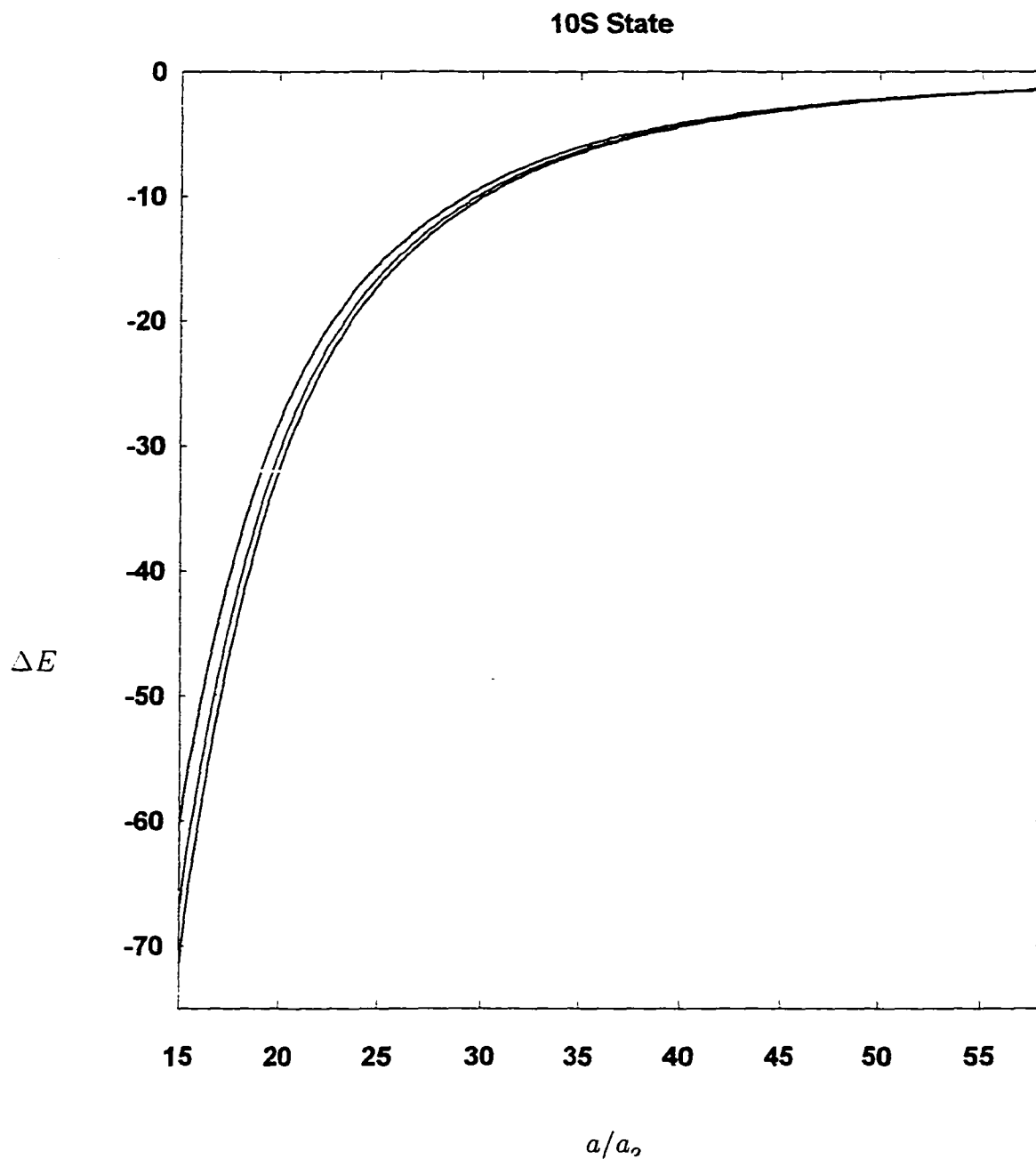


Figure 9. Self-energy (in eV) of a hydrogen atom, in the 10S excited state, as a function of the gap with the nucleus set at $z_2 = 0$. The red, green and blue curves are for $r_s = 1.88$, $r_s = 3.02$ and $r_s = 5.63$ respectively.

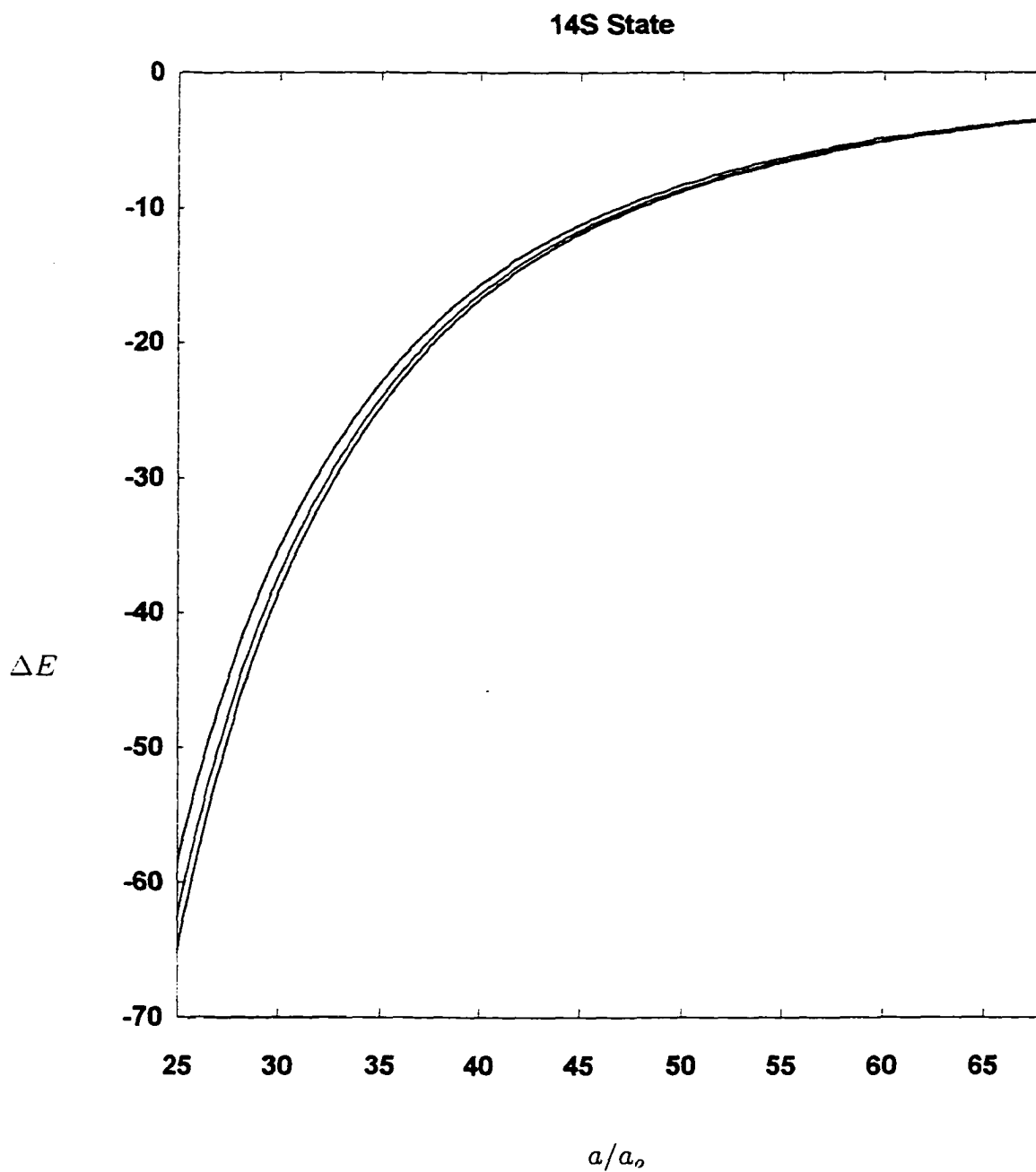


Figure 10. Self-energy (in eV) of a hydrogen atom, in the 14S excited state, as a function of the gap with the nucleus set at $z_2 = 0$. The red, green and blue curves are for $r_s = 1.88$, $r_s = 3.02$ and $r_s = 5.63$ respectively.

5 CONCLUDING REMARKS

In this thesis we have obtained the theoretical expressions for the potential energies of an electron, as well as an atom, enclosed in a cavity between two parallel metal plates. We have used the potential energies as perturbation to obtain the change in the energy of a hydrogen atom when it is at the center of the gap and in its 1S state. Approximate expressions (dipolar approximation) are also obtained for the 3S, 10S and 14S states

The main contribution of the thesis is in its full consideration of the plasmon dispersion when calculating the potential energy of a charged particle (i.e., electron) and the expectation value for the interaction energy between the hydrogen atom and the metal surfaces. It is seen from the diagrams that the potential energy of an electron and electron-nucleus is affected strongly by the dispersion effects, especially when the gap is small. The scattering experiments of an electron by a surface may reveal the validity of the significance of the dispersion effects considered in thesis. The changes in the energy of the hydrogen atom in its 1S state are done considering both the multipolar excitations and the dispersion of the plasmons. It is shown that the effect of dispersion on the energy is large as the gap width is decreased.

A Hydrodynamical Model

The collective motion of electrons in such metals as Na or Al can be studied using the jellium model. In this model the positively charged ions are smeared out uniformly over the crystal and the dynamics of the electrons are studied with the ions providing a static background. The characteristics of the metal are provided completely by n_o , the electron density, or by r_s , the interaction distance given in

$$\frac{4\pi}{3}r_s^3 = \frac{1}{n_o a_o} \quad (\text{A.47})$$

where a_o is the Bohr radius. At equilibrium, the positively charged ions and the electrons will have equal densities at every point. However, if in some particular region the electrons are displaced locally, the imbalance of charge will create an excess of positive charge. The Coulomb attraction will pull the electrons back into the region, however, they will overshoot and oscillations will take place. The frequency of these plasma oscillations, called the plasma frequency, depends on the electron mass m_e , elementary charge e , and n_o and is given by

$$\omega_p^2 = \frac{4\pi n_o e^2}{m_e}. \quad (\text{A.48})$$

For a typical metal, eqn. (48) yields approximately $10^{16} s^{-1}$ compared to $10^{13} s^{-1}$ for lattice

vibrations.

In 1933-34, Bloch provided the hydrodynamical model of bulk and surface modes for the metal electrons. This theory applies to the dynamics of a continuous electron fluid and leads to the bulk and surface plasmons. The bulk modes have amplitudes that extend throughout the electron fluid while the amplitude of the surface modes decay exponentially with position from the surface. The variation of mode frequencies with wave number or spatial dispersion, is the result of the hydrodynamic pressure of the fluid.

The electron fluid has mass density $m_e(n + \Delta n)$, charge density $e(n + \Delta n)$ and an immobile neutralizing background charge density $-en$. We now develop the equation of motion of the electron fluid which includes the effect of electron pressure. For a 3-D displacement vector $\zeta(\mathbf{r})$ of the fluid, the change in the electron density is given by

$$\Delta n = -n_o \nabla \cdot \zeta. \quad (\text{A.49})$$

The deviation of the hydrodynamic pressure from its equilibrium value is

$$\Delta p = -n_o m_e \beta^2 \nabla \cdot \zeta \quad (\text{A.50})$$

where β is a parameter. Poisson's equation governs the electric field inside the plasma

$$E = -\nabla\zeta \quad \text{and} \quad \nabla^2\Phi = 4\pi ne\nabla \cdot \zeta, \quad (\text{A.51})$$

and if the force per unit volume is $neE - \nabla(\Delta p)$, the equation of motion can be written

$$m_e n_o \frac{\partial^2 \zeta}{\partial t^2} = \nabla (n_o e \Phi - n_o m_e \beta^2 \nabla \cdot \zeta) \quad \text{or}$$

$$m_e \frac{\partial^2 \zeta}{\partial t^2} = \nabla (e \Phi - m_e \beta^2 \nabla \cdot \zeta). \quad (\text{A.52})$$

and for normal modes having time dependence $e^{-i\omega t}$, eqn. (52) would read

$$m_e \omega^2 \zeta = \nabla (e \Phi - m_e \beta^2 \nabla \cdot \zeta). \quad (\text{A.53})$$

We now define a displacement potential Ψ first introduced by Barton, which is the basic variable,

$$\zeta = -\nabla\Psi, \quad (\text{A.54})$$

and when substituted into eqn. (53) and integrating once gives

$$-m_e \omega^2 \nabla \Psi = \nabla (e\Phi + m_e \beta^2 \nabla^2 \Psi) \quad \text{or}$$

$$-m_e \omega^2 \Psi = e\Phi + m_e \beta^2 \nabla^2 \Psi. \quad (\text{A.55})$$

Equation (55) can now be rearranged to obtain

$$\Phi = -\frac{m_e}{e} (\omega^2 + \beta^2 \nabla^2) \Psi \quad z \leq 0 \quad (\text{A.56})$$

and if we operate on both side with ∇^2 and use eqn. (51), the basic differential equation for the plasma normal modes is

$$4\pi n e \nabla \cdot \zeta = -\frac{m_e}{e} \omega^2 \nabla^2 \Psi + \beta^2 \nabla^4 \Psi$$

$$4\pi n e \nabla^2 \Psi = -\frac{m_e}{e} \omega^2 \nabla^2 \Psi + \beta^2 \nabla^4 \Psi \quad \text{or}$$

$$0 = \nabla^2 (\omega^2 - \omega_p^2 + \beta^2 \nabla^2) \Psi \quad (\text{A.57})$$

where eqn. (??), the square of the plasma frequency was used. Outside of the plasma, i.e.

$z > 0$. eqn. (51) reads

$$\nabla^2 \Phi = 0. \quad (\text{A.58})$$

In specifying the boundary conditions, the exponential increase is ruled out and we only consider the natural hydrodynamical condition which is that the normal component of the displacement vanishes and which gives

$$\zeta_z = 0 = \frac{\partial \Psi}{\partial z} \quad \text{at } z = 0_- \quad (\text{A.59})$$

and by using eqns. (51) and (53), is equivalent to

$$\frac{\partial}{\partial z} (e\Phi + m_e \beta^2 \nabla^2 \Psi) = 0 \quad \text{at } z = 0_-. \quad (\text{A.60})$$

The above boundary conditions allow the volume charge density to remain non-zero at the surface. The standard boundary conditions for the electric field and pressure are

$$\Phi \quad \text{and} \quad \frac{\partial \Phi}{\partial z} \quad \text{are continuous across } z = 0. \quad (\text{A.61})$$

The individual modes can be written in complex notation as

$$\Psi(r) = e^{ik \cdot \rho} \psi(z) \quad \text{and} \quad \Phi(r) = e^{ik \cdot \rho} \varphi(z) \quad (\text{A.62})$$

where $r = (\rho, z)$ and, like k , ρ is a two component vector parallel to the surface which implies translational invariance. Using (62), we find that inside of the plasma, eqns. (56) and (57) become respectively

$$-\frac{e}{m_e} \varphi = \left(\omega^2 - \beta^2 k^2 + \beta^2 \frac{d^2}{dz^2} \right) \psi \quad (\text{A.63})$$

and

$$\left(-k^2 + \frac{d^2}{dz^2} \right) \left(\omega^2 - \omega_p^2 + \beta^2 k^2 - \beta^2 \frac{d^2}{dz^2} \right) \psi = 0, \quad (\text{A.64})$$

and outside of the plasma we obtain from Laplaces equation (58),

$$\varphi = \text{const} \times \exp(-kz) \quad z \leq 0. \quad (\text{A.65})$$

Applying the boundary conditions (59) to (61) when $\omega^2 < \omega_p^2 + \beta^2 k^2$, the solution to eqn. (64) for surface modes is of the form

$$\psi(z) = N_k \left(p_s e^{kz} - k e^{p_s z} \right), \quad (\text{A.66})$$

where N_k is a normalization constant and p_s is defined by

$$\omega_s^2 = \omega_p^2 + \beta^2 k^2 - \beta^2 p_s^2. \quad (\text{A.67})$$

To determine ω_s from (66), eqns. (63) and (65) are used with boundary conditions (61) to obtain

$$\omega_s^2 = \frac{1}{2} \left(\omega_p^2 + \beta^2 k^2 + \beta k \sqrt{2\omega_p^2 + \beta^2 k^2} \right), \quad (\text{A.68})$$

which is the normal surface mode frequency for one surface. The procedure for two surfaces is done in a similar manner to give eqn. (7).

B Interaction Energy Integrals

In this appendix we provide the analytical values of the integrals used in the averaging process in obtaining the interaction energy for all three regions of the system. In region I, I_1 , $I_{2\pm}$ and $I_{3\pm}$ of eqn. (39) are integrated analytically using

$$\langle e^{\xi z} \rangle = \int_0^{-a-z_2} \int_0^\infty \int_0^{2\pi} \frac{\alpha^3}{\pi} e^{\xi z} e^{-2\alpha\sqrt{R^2+z^2}} R dR d\phi dz \quad (\text{B.69})$$

where ξ takes on values $2k$ for I_1 , $(k + \gamma_\pm)$ for $I_{2\pm}$ and $2\gamma_\pm$ for $I_{3\pm}$ and $z = z_1 - z_2$. From the above we obtain

$$\begin{aligned} I_1 &= e^{2k(z_2+a)} \langle e^{2kz} \rangle \\ &= \frac{e^{-2\alpha(a+z_2)}}{2(\alpha+k)} \left(\frac{\alpha}{2} + \alpha^2(a+z_2) + \frac{\alpha^2}{2(\alpha+k)} \right), \end{aligned} \quad (\text{B.70})$$

$$\begin{aligned} I_{2\pm} &= e^{(k+\gamma_\pm)(z_2+a)} \langle e^{(k+\gamma_\pm)z} \rangle \\ &= \frac{e^{-2\alpha(a+z_2)}}{2\alpha+k+\gamma_\pm} \left(\frac{\alpha}{2} + \alpha^2(a+z_2) + \frac{\alpha^2}{2\alpha+k+\gamma_\pm} \right), \end{aligned} \quad (\text{B.71})$$

$$\begin{aligned}
I_{3\pm} &= e^{2\gamma_{\pm}(z_2+a)} \langle e^{2\gamma_{\pm}z} \rangle \\
&= \frac{e^{-2\alpha(a+z_2)}}{2(\alpha + \gamma_{\pm})} \left(\frac{\alpha}{2} + \alpha^2(a + z_2) + \frac{\alpha^2}{2(\alpha + \gamma_{\pm})} \right). \tag{B.72}
\end{aligned}$$

For J_1 and $J_{2\pm}$ in eqn. (40), we use

$$\langle e^{\xi z + ik \cdot R} \rangle = \int_{-\infty}^{-z_2+a} \int_0^{\infty} \int_0^{2\pi} \frac{\alpha^3}{\pi} e^{\xi z + ik \cdot R} e^{-2\alpha\sqrt{R^2+z^2}} R dR d\phi dz \tag{B.73}$$

where ξ takes the values k for J_1 and γ_{\pm} for $J_{2\pm}$ which results in

$$\begin{aligned}
J_1 &= e^{2k(z_2+a)} \langle e^{kz + ik \cdot R} \rangle \\
&= \frac{\alpha^4 e^{-(z_2+a)\sqrt{4\alpha^2+k^2}}}{(4\alpha^2 + k^2) (k + \sqrt{4\alpha^2 + k^2})} \\
&\quad \times \left(\frac{1}{\sqrt{4\alpha^2 + k^2}} + \frac{1}{k + \sqrt{4\alpha^2 + k^2}} + z_2 + a \right) \tag{B.74}
\end{aligned}$$

$$J_{2\pm} = e^{2k(z_2+a)} \langle e^{kz + ik \cdot R} \rangle$$

$$\begin{aligned}
&= \frac{\alpha^4 e^{-(z_2+a)\sqrt{4\alpha^2+k^2}}}{(4\alpha^2+k^2)(\gamma_{\pm}+\sqrt{4\alpha^2+k^2})} \\
&\quad \left(\frac{1}{\sqrt{4\alpha^2+k^2}} + \frac{1}{\gamma_{\pm}+\sqrt{4\alpha^2+k^2}} + z_2+a \right). \tag{B.75}
\end{aligned}$$

Similarly, the integrals used in the averaging process for eqns. (41) to (46) are obtained in the same manner and are stated below:

$$\begin{aligned}
K_1 &= -\alpha^2 \frac{e^{-2\alpha(a+z_2)-2ka}}{2(\alpha+k)} \left(\frac{1}{2\alpha} + \frac{1}{2(\alpha+k)} + a+z_2 \right) \\
&\quad -\alpha^2 \frac{e^{2kz_2}}{2(\alpha+k)} \left(\frac{1}{2\alpha} + \frac{1}{2(\alpha+k)} \right) \\
&\quad -\alpha^2 \frac{e^{-2\alpha(a-z_2)+2ka}}{2(\alpha-k)} \left(\frac{1}{2\alpha} + \frac{1}{2(\alpha-k)} + a-z_2 \right) \\
&\quad -\alpha^2 \frac{e^{2kz_2}}{2(\alpha-k)} \left(\frac{1}{2\alpha} + \frac{1}{2(\alpha-k)} \right) \tag{B.76}
\end{aligned}$$

$$K_2 = -\alpha^2 \frac{e^{-2\alpha(a+z_2)+2ka}}{2(\alpha-k)} \left(\frac{1}{2\alpha} + \frac{1}{2(\alpha-k)} + a+z_2 \right)$$

$$\begin{aligned}
& -\alpha^2 \frac{e^{-2kz_2}}{2(\alpha - k)} \left(\frac{1}{2\alpha} + \frac{1}{2(\alpha - k)} \right) \\
& -\alpha^2 \frac{e^{-2\alpha(a-z_2)-2ka}}{2(\alpha + k)} \left(\frac{1}{2\alpha} + \frac{1}{2(\alpha + k)} + a - z_2 \right) \\
& -\alpha^2 \frac{e^{-2kz_2}}{2(\alpha + k)} \left(\frac{1}{2\alpha} + \frac{1}{2(\alpha + k)} \right)
\end{aligned} \tag{B.77}$$

$$K_3 = -\alpha^2 \left[\frac{e^{-2\alpha(a+z_2)}}{2\alpha} \left(\frac{1}{\alpha} + a + z_2 \right) - \frac{e^{-2\alpha(a-z_2)}}{2\alpha} \left(\frac{1}{\alpha} + a - z_2 \right) - \frac{1}{\alpha^2} \right] \tag{B.78}$$

$$\begin{aligned}
L_1 = & -\frac{4\alpha^4}{4\alpha^2 + k^2} \frac{e^{-a(\sqrt{4\alpha^2+k^2}-k)} \left(\frac{1}{\sqrt{4\alpha^2+k^2}} + \frac{1}{\sqrt{4\alpha^2+k^2}-k} + a + z_2 \right)}{\sqrt{4\alpha^2+k^2}-k} \\
& + \frac{4\alpha^4}{4\alpha^2 + k^2} \frac{e^{-kz_2} \left(\frac{1}{\sqrt{4\alpha^2+k^2}} + \frac{1}{\sqrt{4\alpha^2+k^2}-k} \right)}{\sqrt{4\alpha^2+k^2}-k} \\
& - \frac{4\alpha^4}{4\alpha^2 + k^2} \frac{e^{-a(\sqrt{4\alpha^2+k^2}+k)} \left(\frac{1}{\sqrt{4\alpha^2+k^2}} + \frac{1}{\sqrt{4\alpha^2+k^2}+k} + a - z_2 \right)}{\sqrt{4\alpha^2+k^2}+k} \\
& + \frac{4\alpha^4}{4\alpha^2 + k^2} \frac{e^{-kz_2} \left(\frac{1}{\sqrt{4\alpha^2+k^2}} + \frac{1}{\sqrt{4\alpha^2+k^2}+k} \right)}{\sqrt{4\alpha^2+k^2}+k}
\end{aligned} \tag{B.79}$$

$$\begin{aligned}
L_2 = & -\frac{4\alpha^4}{4\alpha^2 + k^2} \frac{e^{-a(\sqrt{4\alpha^2+k^2}+k)} \left(\frac{1}{\sqrt{4\alpha^2+k^2}} + \frac{1}{\sqrt{4\alpha^2+k^2}+k} + a + z_2 \right)}{\sqrt{4\alpha^2 + k^2} + k} \\
& + \frac{4\alpha^4}{4\alpha^2 + k^2} \frac{e^{kz_2} \left(\frac{1}{\sqrt{4\alpha^2+k^2}} + \frac{1}{\sqrt{4\alpha^2+k^2}+k} \right)}{\sqrt{4\alpha^2 + k^2} + k} \\
& - \frac{4\alpha^4}{4\alpha^2 + k^2} \frac{e^{-a(\sqrt{4\alpha^2+k^2}-k)} \left(\frac{1}{\sqrt{4\alpha^2+k^2}} + \frac{1}{\sqrt{4\alpha^2+k^2}-k} + a - z_2 \right)}{\sqrt{4\alpha^2 + k^2} - k} \\
& + \frac{4\alpha^4}{4\alpha^2 + k^2} \frac{e^{kz_2} \left(\frac{1}{\sqrt{4\alpha^2+k^2}} + \frac{1}{\sqrt{4\alpha^2+k^2}-k} \right)}{\sqrt{4\alpha^2 + k^2} - k} \tag{B.80}
\end{aligned}$$

$$M_1 = \frac{e^{-2\alpha(a-z_2)}}{2(\alpha+k)} \left(\frac{\alpha}{2} + \alpha^2(a-z_2) + \frac{\alpha^2}{2(\alpha+k)} \right) \tag{B.81}$$

$$M_{2\pm} = \frac{e^{-2\alpha(a-z_2)}}{2\alpha+k+\gamma_{\pm}} \left(\frac{\alpha}{2} + \alpha^2(a-z_2) + \frac{\alpha^2}{2\alpha+k+\gamma_{\pm}} \right) \tag{B.82}$$

$$M_{3\pm} = \frac{e^{-2\alpha(a-z_2)}}{2(\alpha+\gamma_{\pm})} \left(\frac{\alpha}{2} + \alpha^2(a-z_2) + \frac{\alpha^2}{2(\alpha+\gamma_{\pm})} \right) \tag{B.83}$$

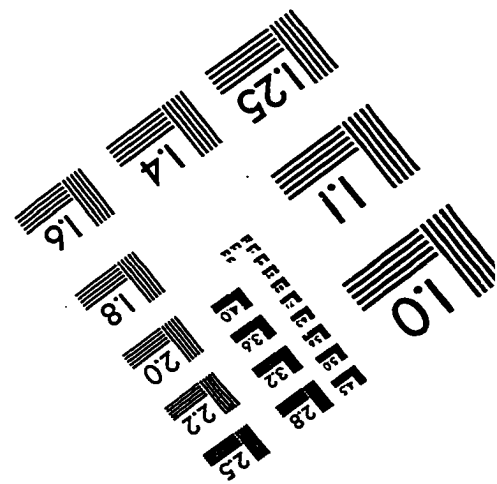
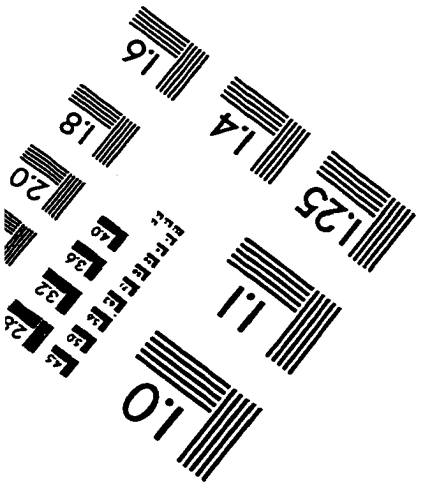
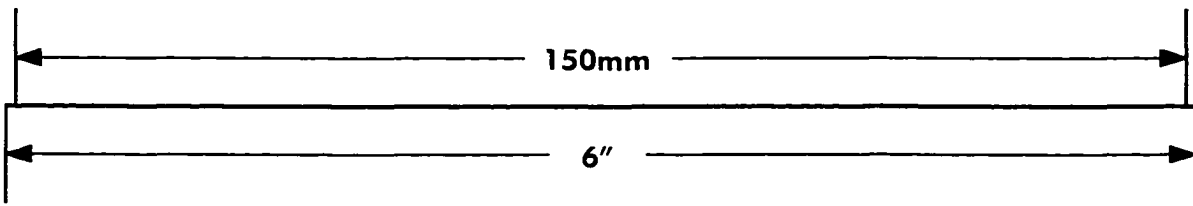
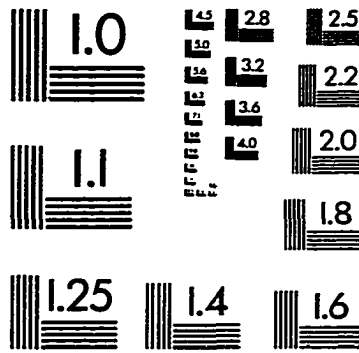
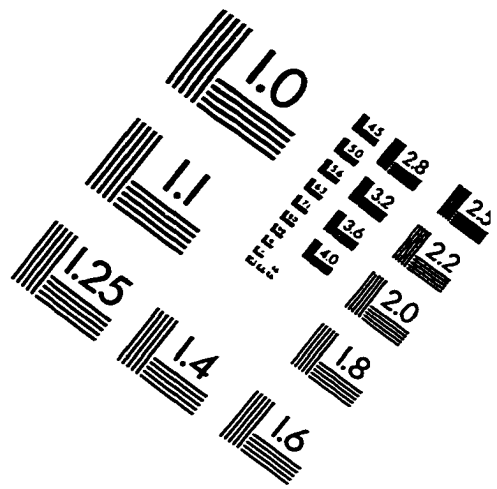
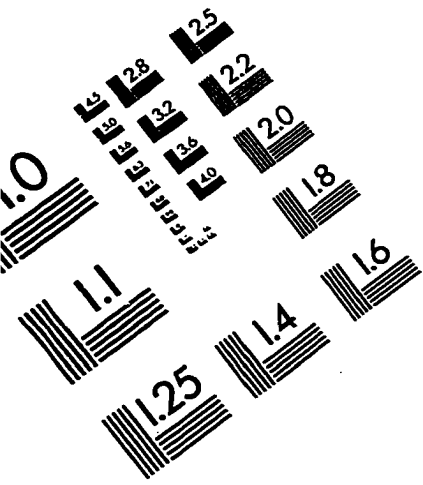
$$\begin{aligned}
N_1 &= \frac{\alpha^4 e^{-(a-z_2)\sqrt{4\alpha^2+k^2}}}{(4\alpha^2+k^2)(k+\sqrt{4\alpha^2+k^2})} \\
&\quad \times \left(\frac{1}{\sqrt{4\alpha^2+k^2}} + \frac{1}{k+\sqrt{4\alpha^2+k^2}} - z_2 + a \right), \tag{B.84}
\end{aligned}$$

$$\begin{aligned}
N_{2\pm} &= \frac{\alpha^4 e^{-(a-z_2)\sqrt{4\alpha^2+k^2}}}{(4\alpha^2+k^2)(\gamma_{\pm}+\sqrt{4\alpha^2+k^2})} \\
&\quad \times \left(\frac{1}{\sqrt{4\alpha^2+k^2}} + \frac{1}{\gamma_{\pm}+\sqrt{4\alpha^2+k^2}} - z_2 + a \right). \tag{B.85}
\end{aligned}$$

References

- [1] N. D. Lang and W. Kohn. Phys. Rev.. B1, 4555, 1970.
- [2] G. D. Mahan. Collective Properties of Physical Systems. Academic Press, 1973.
- [3] E. M. Chan, M. J. Buckingham and J. L. Robin. Surf. Sci., 67, 285, 1977.
- [4] F. Bloch, Z. Phys., 81, 363, 1933.
- [5] G. Barton. Rep. Prog. Phys., 42, 963, 1979.
- [6] K. N. Pathak, V. V. Paranjape and M. R. Monga. Phys. Rev., B40, 9565, 1989.
- [7] B. Singla, K. Dharamvir, K. N. Pathak and V. V. Paranjape. Phys. Rev., B48, 15256, 1993.
- [8] V. Sandoghdar, C. I. Sukenik, E. A. Hinds and Serge Haroche. Phys. Rev. Lett., 68, 3432, 1992.
- [9] F. Soles and R. H. Ritchie. Phys. Rev., B35, 9314, 1987.
- [10] V. V. Paranjape, P. V. Panat and P. K. Pathak. Phys. Rev., B55, 7227, 1997.
- [11] P. M. Platzman. Phys. Rev.. 125. 1961, 1962.

IMAGE EVALUATION TEST TARGET (QA-3)



APPLIED IMAGE, Inc
1653 East Main Street
Rochester, NY 14609 USA
Phone: 716/482-0300
Fax: 716/288-5589

© 1993, Applied Image, Inc., All Rights Reserved